

GPS Multipath Detection Based on Carrier-to-Noise-Density Ratio Measurements from a Dual-Polarized Antenna

Sanghyun Kim, Halim Lee, and Kwansik Park*

School of Integrated Technology, Yonsei University,
Incheon, 21983, Korea (sanghyun.kim, halim.lee, KwansikPark@yonsei.ac.kr)

* Corresponding author

Abstract: In this study, the global positioning system (GPS) multipath detection was performed based on the carrier-to-noise-density ratio, C/N_0 , measured through a dual-polarized antenna. As the right hand circular polarization (RHCP) antenna is sensitive to the signals directly received from the GPS, and the left hand circular polarization (LHCP) antenna is sensitive to the singly reflected signals, the C/N_0 difference between the RHCP and LHCP measurements is used for multipath detection. Once we collected the GPS signals in a low multipath location, we calculated the C/N_0 difference to obtain a threshold value that can be used to detect the multipath GPS signal received from another location. The results were validated through a ray-tracing simulation.

Keywords: multipath detection, global positioning system, carrier-to-noise-density ratio, dual-polarized antenna

1. INTRODUCTION

In order to obtain positioning, navigation, and timing (PNT) information [1–10], the demand for global navigation satellite systems (GNSSs), in particular the global positioning system (GPS) [11–16], is increasing in various applications such as ground vehicles, air/marine transport, unmanned aerial vehicles (UAVs), and robots [17–27]. Thanks to multi-constellation and multi-frequency GNSS technology, the positioning accuracy and availability significantly improved [28, 29]. However, buildings can easily reflect and block the GNSS signals. A user may receive both line-of-sight (LOS) and non-line-of-sight (NLOS) GNSS signals simultaneously (i.e., *LOS+NLOS condition*), or only NLOS signals may be received (i.e., *NLOS-only condition*) [30–33]. These phenomena can reduce positioning accuracy and availability in urban environments and may lead to a positioning error of more than 100 m [34].

There are many proposed methods to detect LOS+NLOS or NLOS-only signals. For example, some special antennas, such as dual-polarized antenna or array antenna, a 3D city model, a sky-pointing camera, and several algorithm-based methods based on GNSS measurements could be used to detect LOS+NLOS or NLOS-only signals [35–39]. In this study, we performed the GPS multipath detection (i.e., both LOS+NLOS and NLOS-only detection) based on the carrier-to-noise-density ratio (C/N_0) measurements through a dual-polarized antenna, which was proposed in [35]. The GPS signals received directly from the satellites have a right hand circular polarization (RHCP), while the singly reflected signals have a left hand circular polarization (LHCP) or an elliptical polarization [40, 41]. The RHCP and LHCP antennas are sensitive to the RHCP and LHCP signals, respectively. Therefore, the C/N_0 difference between the RHCP and LHCP measurements depends on the multipath condition.

We obtained the elevation-dependent threshold for

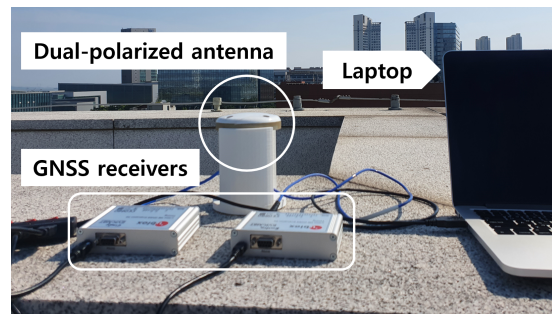


Fig. 1. Hardware setup installed on the rooftop for the experiments

the LOS+NLOS and NLOS-only detection based on the C/N_0 difference value measured in a low multipath environment. If the C/N_0 difference of the observed GPS signal is lower than the threshold at a given elevation, the observed GPS signal is likely to be multipath-contaminated. If a multipath-contaminated signal was detected in this way, we performed a ray-tracing simulation using a commercial ray-tracing software to validate the results. By observing the propagation paths of the received GPS signals obtained through ray-tracing, we can confirm the existence of multipath signals. However, the previous study in [35] did not quantitatively validate the existence of multipath signals through a ray-tracing simulation but qualitatively explained the multipath environment. In this study, we generated the ground truth of the existence of multipath signals through a ray-tracing simulation for proper evaluation of the multipath detection method.

2. EXPERIMENT SETUP

2.1 GPS signals collection

Fig. 1 shows the hardware setup consisting of a dual-polarized antenna produced by Antcom, a pair of u-blox EVK-M8T GNSS receivers, and a laptop to collect GPS



Fig. 2. GPS signals collection on the rooftop of the building

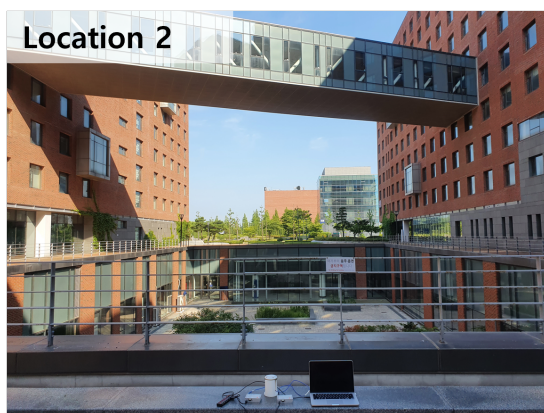


Fig. 3. GPS signals collection in location 2 surrounded by buildings

signals. The experiments were conducted at Yonsei University, Incheon, Korea, in two locations, shown in Figs. 2 and 3. Location 1 is the rooftop of the building, which has a low multipath environment, while location 2 is surrounded by buildings and can be heavily influenced by multipath. We collected GPS L1 signals at these locations, and the C/N_0 measurements were collected every 1 s and quantized at 1 dB intervals.

2.2 Ray-tracing simulation

The multipath detection performance was validated through the ray-tracing simulation using a commercial 3D building map from 3dbuildings [42] and a commercial ray-tracing software called Wireless InSite [43]. Fig. 4 represents the 3D building map of Yonsei University, Incheon, Korea and surrounding areas imported in the Wireless InSite software. The locations of the GPS satellites were set based on almanac information. It was assumed that the signals collected by the receiver were reflected two times maximum to reduce the computational complexity of the simulation. The existence of GPS multipath signals can be confirmed by observing the propagation paths of the GPS signals after the ray-tracing.

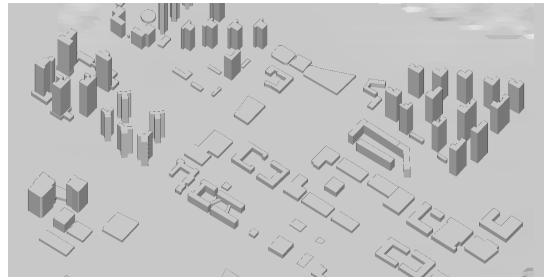


Fig. 4. 3D building map imported in the ray-tracing software

3. RESULTS

The C/N_0 difference values of the RHCP and LHCP measurements were obtained as the green data points in Fig. 5, which is the case of the PRN 13 satellite as an example. Similarly, we can plot the measured C/N_0 difference values of all PRNs from location 1 (i.e., low multipath environment) according to the elevation of 10° to 35° as in Fig. 6. Even in the low-multipath environment, the C/N_0 difference varied according to the elevation angles. As the elevation-dependent multipath detection threshold, we calculated the mean of C/N_0 difference values at each elevation. The determined threshold is the red curve in Fig. 6.

For the data collected at location 2, the measured C/N_0 difference was compared with the multipath detection threshold at the corresponding elevation angle. If the measured C/N_0 difference is lower than the threshold, the signal is determined to be contaminated by multipath. Fig. 7 shows the measured C/N_0 difference values of PRN 13 and PRN 9 from location 2 and the threshold as an example. Because most data points lie below the threshold, the signals from the PRN 13 and PRN 9 satellites are likely to be affected by multipath.

Finally, to validate whether the PRN 13 and PRN 9 signals were really affected by multipath, ray-tracing simulation was performed. By ray-tracing, it is able to predict the signal reflection and blockage due to buildings. Figs. 8 and 9 show the propagation paths of the PRN 13 and PRN 9 signals received at location 2, respectively. It is confirmed that, in both cases, there were not only the LOS signal, but also three or four NLOS signals reflected by the buildings (i.e., LOS+NLOS condition).

4. CONCLUSION

In this study, we performed the GPS multipath detection based on the measurements of C/N_0 from a dual-polarized antenna. We calculated the C/N_0 difference between the RHCP and LHCP antenna components in the low multipath location to obtain the elevation-dependent multipath detection threshold. When the C/N_0 of a certain GPS signal is lower than the threshold at the corresponding elevation angle, the signal is likely to be contaminated by multipath. Finally, we verified the multipath detection results through a ray-tracing simulation. As a

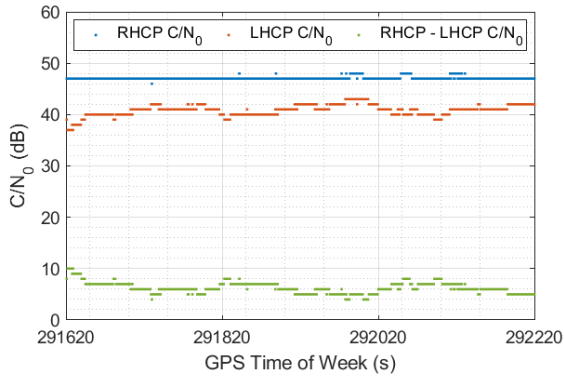


Fig. 5. Measured C/N_0 using a dual-polarized antenna from location 1 (PRN 13)

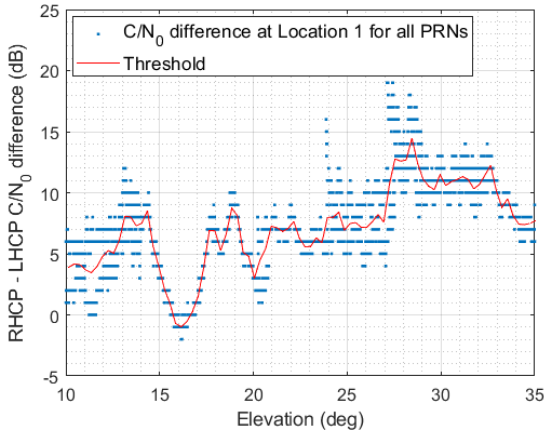


Fig. 6. Measured C/N_0 difference from location 1 for all PRNs and multipath detection threshold

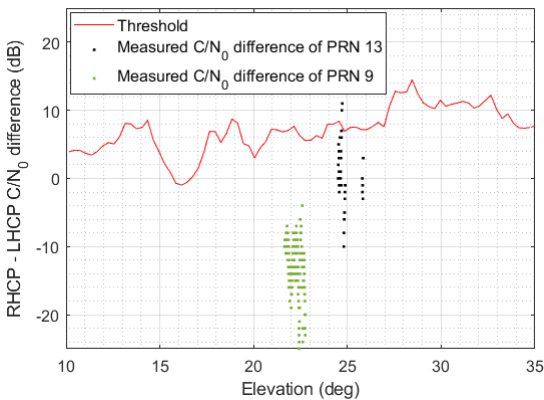


Fig. 7. Measured C/N_0 difference of PRN 13 and PRN 9 from location 2 compared with the threshold

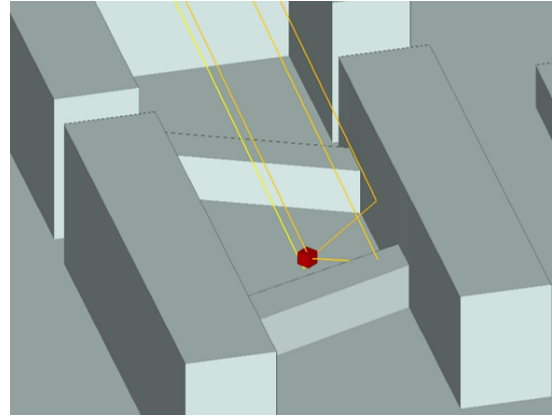


Fig. 8. The propagation paths of the PRN 13 signals received at location 2

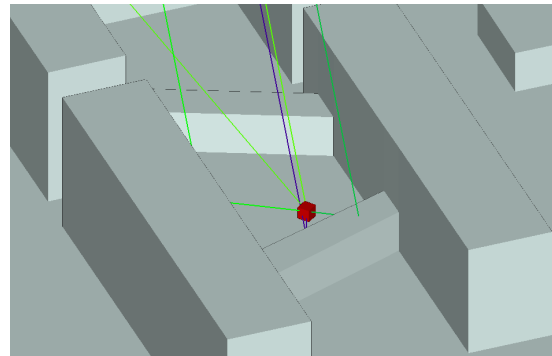


Fig. 9. The propagation paths of the PRN 9 signals received at location 2

future work, a generalized multipath detection method based on a machine learning technique using various GNSS measurements can be studied.

ACKNOWLEDGEMENT

This research was supported by the Unmanned Vehicles Core Technology Research and Development Program through the National Research Foundation of Korea (NRF) and the Unmanned Vehicle Advanced Research Center (UVARC) funded by the Ministry of Science and ICT, Republic of Korea (2020M3C1C1A01086407).

REFERENCES

- [1] K. Park, W. Kim, and J. Seo, "Effects of initial attitude estimation errors on loosely coupled smartphone GPS/IMU integration system," in *Proc. IC-CAS*, Oct. 2020, pp. 800–803.
- [2] H. Yoon, H. Seok, C. Lim, and B. Park, "An on-line SBAS service to improve drone navigation performance in high-elevation masked areas," *Sensors*, vol. 20, no. 11, 2020.
- [3] S. Jeong, H. Lee, T. Kang, and J. Seo, "RSS-based LTE base station localization using single receiver in environment with unknown path-loss exponent," in *Proc. ICTC*, Oct. 2020, pp. 958–961.

- [4] K. Shamaei and Z. M. Kassas, "A joint TOA and DOA acquisition and tracking approach for positioning with LTE signals," *IEEE Trans. Signal Process.*, vol. 69, pp. 2689–2705, 2021.
- [5] W. Kim, P.-W. Son, J. Rhee, and J. Seo, "Development of record and management software for GPS/Loran measurements," in *Proc. ICCAS*, Oct. 2020, pp. 796–799.
- [6] M. Maaref and Z. M. Kassas, "Ground vehicle navigation in GNSS-challenged environments using signals of opportunity and a closed-loop map-matching approach," *IEEE Trans. Intell. Transp. Syst.*, vol. 21, no. 7, pp. 2723–2738, 2020.
- [7] J. Park, P.-W. Son, W. Kim, J. Rhee, and J. Seo, "Effect of outlier removal from temporal ASF corrections on multichain Loran positioning accuracy," in *Proc. ICCAS*, Oct. 2020, pp. 824–826.
- [8] P.-W. Son, J. Rhee, J. Hwang, and J. Seo, "Universal kriging for Loran ASF map generation," *IEEE Trans. Aerosp. Electron. Syst.*, vol. 55, no. 4, pp. 1828–1842, Oct. 2019.
- [9] S. Han, T. Kang, and J. Seo, "Smartphone application to estimate distances from LTE base stations based on received signal strength measurements," in *Proc. ITC-CSCC*, Jun. 2019.
- [10] J. H. Rhee, S. Kim, P.-W. Son, and J. Seo, "Enhanced accuracy simulator for a future Korean nationwide eLoran system," *IEEE Access*, in press.
- [11] E. Schmidt, N. Gatsis, and D. Akopian, "A GPS spoofing detection and classification correlator-based technique using the LASSO," *IEEE Trans. Aerosp. Electron. Syst.*, vol. 56, no. 6, pp. 4224–4237, 2020.
- [12] K. Park and J. Seo, "Single-antenna-based GPS antijamming method exploiting polarization diversity," *IEEE Trans. Aerosp. Electron. Syst.*, vol. 57, no. 2, pp. 919–934, Apr. 2021.
- [13] M. Braasch and A. Dempster, "Tutorial: GPS receiver architectures, front-end and baseband signal processing," *IEEE Aerosp. Electron. Syst. Mag.*, vol. 34, no. 2, pp. 20–37, 2019.
- [14] K. Park, D. Lee, and J. Seo, "Dual-polarized GPS antenna array algorithm to adaptively mitigate a large number of interference signals," *Aerosp. Sci. Technol.*, vol. 78, pp. 387–396, Jul. 2018.
- [15] S. Kim, K. Park, and J. Seo, "Mitigation of GPS chirp jammer using a transversal FIR filter and LMS algorithm," in *Proc. ITC-CSCC*, Jun. 2019.
- [16] V. L. Knoop, P. F. de Bakker, C. C. J. M. Tiberius, and B. van Arem, "Lane determination with GPS precise point positioning," *IEEE Trans. Intell. Transp. Syst.*, vol. 18, no. 9, pp. 2503–2513, 2017.
- [17] S. Kim, J. Park, J.-K. Yun, and J. Seo, "Motion planning by reinforcement learning for an unmanned aerial vehicle in virtual open space with static obstacles," in *Proc. ICCAS*, Oct. 2020, pp. 784–787.
- [18] K. Sun, H. Chang, J. Lee, J. Seo, Y. Jade Mor-ton, and S. Pullen, "Performance benefit from dual-frequency GNSS-based aviation applications under ionospheric scintillation: A new approach to fading process modeling," in *Proc. ION ITM*, Jan. 2020, pp. 889–899.
- [19] F. Causa and G. Fasano, "Improving navigation in GNSS-challenging environments: Multi-UAS cooperation and generalized dilution of precision," *IEEE Trans. Aerosp. Electron. Syst.*, vol. 57, no. 3, pp. 1462–1479, 2021.
- [20] H.-S. Moon and J. Seo, "Prediction of human trajectory following a haptic robotic guide using recurrent neural networks," in *Proc. IEEE World Haptics Conf. (IEEE WHC)*, Aug. 2019, pp. 157–162.
- [21] —, "Optimal action-based or user prediction-based haptic guidance: Can you do even better?" in *Proc. ACM Conf. Human Factors Computing Sys. (ACM CHI)*, no. 281, 2021, pp. 1–12.
- [22] —, "Dynamic difficulty adjustment via fast user adaptation," in *Adjun. Publ. Annu. ACM Sym. User Interface Softw. Technol. (ACM UIST)*, Oct. 2020, pp. 13–15.
- [23] H. Lee, T. Kang, and J. Seo, "Development of confidence bound visualization tool for LTE-based UAV surveillance in urban areas," in *Proc. ICCAS*, Oct. 2019, pp. 1187–1191.
- [24] H. Lee, W. Kim, and J. Seo, "Simulation of UWB radar-based positioning performance for a UAV in an urban area," in *Proc. IEEE ICCE-Asia*, Jun. 2018.
- [25] C. Savas, G. Falco, and F. Dovis, "A comparative performance analysis of GPS L1 C/A, L5 acquisition and tracking stages under polar and equatorial scintillations," *IEEE Trans. Aerosp. Electron. Syst.*, vol. 57, no. 1, pp. 227–244, 2021.
- [26] H.-S. Moon and J. Seo, "Observation of human response to a robotic guide using a variational autoencoder," in *Proc. IEEE IRC*, Feb. 2019, pp. 258–261.
- [27] H.-S. Moon, W. Kim, S. Han, and J. Seo, "Observation of human trajectory in response to haptic feedback from mobile robot," in *Proc. ICCAS*, Oct. 2018, pp. 1530–1534.
- [28] X. Li, M. Ge, X. Dai, X. Ren, M. Fritsche, J. Wickert, and H. Schuh, "Accuracy and reliability of multi-GNSS real-time precise positioning: GPS, GLONASS, BeiDou, and Galileo," *J. Geod.*, vol. 89, no. 6, pp. 607–635, 2015.
- [29] M. Fortunato, J. Critchely-Marrows, M. Siutkowski, M. L. Ivanovici, E. Benedetti, and W. Roberts, "Enabling high accuracy dynamic applications in urban environments using PPP and RTK on android multi-frequency and multi-GNSS smartphones," in *Proc. ENC*, Apr. 2019, pp. 1–9.
- [30] H. Lee and J. Seo, "A preliminary study of machine-learning-based ranging with LTE channel impulse response in multipath environment," in *Proc. IEEE ICCE-Asia*, Nov. 2020.
- [31] H. Lee, A. Abdallah, J. Park, J. Seo, and Z. Kassas,

- “Neural network-based ranging with LTE channel impulse response for localization in indoor environments,” in *Proc. ICCAS*, Oct. 2020, pp. 939–944.
- [32] M. Jia, H. Lee, J. Khalife, Z. M. Kassas, and J. Seo, “Ground vehicle navigation integrity monitoring for multi-constellation GNSS fused with cellular signals of opportunity,” in *Proc. IEEE ITSC*, 2021.
- [33] H. Lee, J. Seo, and Z. Kassas, “Integrity-based path planning strategy for urban autonomous vehicular navigation using GPS and cellular signals,” in *Proc. ION GNSS+*, Sep. 2020, pp. 2347–2357.
- [34] G. MacGougan, G. Lachapelle, R. Klukas, K. Siu, L. Garin, J. Shewfelt, and G. Cox, “Performance analysis of a stand-alone high-sensitivity receiver,” *GPS Solut.*, vol. 6, no. 3, pp. 179–195, 2002.
- [35] P. Groves, Z. Jiang, B. Skelton, P. Cross, L. Lau, Y. Adane, and I. Kale, “Novel multipath mitigation methods using a dual-polarization antenna,” in *Proc. ION GNSS*, Sep. 2010, pp. 140–151.
- [36] R. Sun, L. Fu, G. Wang, Q. Cheng, and L. T. Hsu, “Using dual-polarization GPS antenna with optimized adaptive neuro-fuzzy inference system to improve single point positioning accuracy in urban canyons,” *Navig. J. Inst. Navig.*, vol. 68, no. 1, pp. 41–60, 2021.
- [37] R. Kumar and M. G. Petovello, “A novel GNSS positioning technique for improved accuracy in urban canyon scenarios using 3D city model,” in *Proc. ION GNSS+*, Sep. 2014, pp. 2139–2148.
- [38] X. Bai, W. Wen, and L. T. Hsu, “Using sky-pointing fish-eye camera and LiDAR to aid GNSS single-point positioning in urban canyons,” *IET Intel. Transport Syst.*, vol. 14, no. 8, pp. 908–918, 2020.
- [39] Y. Lee and B. Park, “Seamless accurate positioning in deep urban area using DGNSS and CMC-based multipath mitigation,” in *Proc. ION GNSS+*, Sep. 2020, pp. 1690–1719.
- [40] M. Brenneman, J. Morton, C. Yang, and F. van Graas, “Mitigation of GPS multipath using polarization and spatial diversities,” in *Proc. ION GNSS*, Sep. 2007, pp. 1221–1229.
- [41] P. Groves, Z. Jiang, M. Rudi, and P. Strode, “A portfolio approach to NLOS and multipath mitigation in dense urban areas,” in *Proc. ION GNSS+*, Sep. 2013, pp. 3231–3247.
- [42] 3Dbuildings. <https://3dbuildings.com/>.
- [43] Remcom. Wireless InSite.